Epoxy-Diamine Thermoset/Thermoplastic Blends: Dielectric Properties before, during, and after Phase Separation

A. Bonnet, J. P. Pascault, and H. Sautereau

Laboratoire des Matériaux Macromoléculaires, UMR - CNRS 5627, Institut National des Sciences Appliquées, 20, Avenue A. Einstein, 69621 Villeurbanne Cedex, France

J. Rogozinski and D. Kranbuehl*

Departments of Chemistry and Applied Science, College of William and Mary, Williamsburg, Virginia 23187-8795

Received August 12, 1999

ABSTRACT: Frequency dependent dielectric measurements have been used to monitor the complex chemical, composition and morphological changes occurring during cure of a high-temperature epoxy−amine (DGEBA−MCDEA) polyetherimide (PEI) blend. The dielectric measurements are able to monitor in situ the reaction advancement before phase separation, the onset of phase separation, the Maxwell−Wagner−Sillars (MWS) effect, and the buildup in T_g in both the continuous thermoplastic PEI-rich phase and the occluded epoxy-rich phase. The MWS predicted values were in relatively good agreement with the experimental values and suggest a nonspherical shape. The conductivity in the homogeneous blend decreased much more rapidly than expected based on concentration and change in viscosity, suggesting that the conduction mechanism in the homogeneous blend is strongly affected by the proximity of the hydrogen-bonding groups in the epoxy amine.

Introduction

Thermoset (TS)/thermoplastic (TP) blends are materials resulting from the mixing of the TP polymer with the TS precursor (generally a diepoxy−diamine system).[1−7] Usually the mixture is initially homogeneous. With time and temperature there is an increase in the molar mass of the TS precursor as the TS reaction advances. A liquid−liquid phase separation occurs at a given conversion. The phase separation process generally continues until the TP-rich phase becomes rich enough to form a glass. The overall process is stopped when the TS is fully reacted or both phases have achieved the glassy state.

These TS/TP blends have two main applications: (i) toughness improvement of TS networks with high performance ductile thermoplastics and (ii) new processing routes which reduce the initial viscosity of otherwise intractable high temperature TP polymers such as polyphenylene ether and polyetherimide. The first application occurs at low concentrations <20 wt % of TP. The second application involves TP concentrations generally greater than 30 wt %. In this case phase inversion occurs resulting in a TP-rich continuous (β) phase with occluded TS-rich (α) phase particles.

This paper focuses on the dielectric behavior of the TP polyetherimide (PEI) and the TS precursor, diglycidyl ether of bisphenol A (DGEBA) reacting with 4,4′-methylenebis[3-chloro-2,6-diethylaniline] (MCDEA). The paper addresses the continuously changing dielectric behavior of the blend before, during, and after the phase separation process. A previous paper has reported results on the reaction kinetics of the TS precursor in the presence of different concentrations of PEI, both before and after phase separation.[8] A second paper reported on the rheological behavior of the blend during reaction.[9]

Previously dielectric measurements have been used to monitor the changing viscosity and buildup in T_g during polymerization of a variety of neat thermoset resins.[10−27] This paper will address the ability of dielectric sensing to monitor these properties both before phase separation in the homogeneous solution and in each phase after the phase separation process. This paper will also discuss the ability of dielectric measurements to detect the onset of phase separation. The viscosity and onset of phase separation are critical processing properties and affect the final morphology. Equally important measurements of the dielectric behavior have the particularly advantage that they can be made easily in both the laboratory and the industrial fabrication environment.

Experimental Section

The TS precursor consisted of an epoxy prepolymer and diamine curing agent. The epoxy prepolymer used was a diglycidyl ether of bisphenol, a liquid at room temperature and with a low degree of polymerization, DGEBA $\bar{n} = 0.15$ (Ref. LY556 from Ciba Geigy). The curing agent was an aromatic diamine with a low reactivity, 4,4′-methylenebis(3-chloro-2,6-diethylaniline), MCDEA, supplied by Lonza. The diamine was used at the stoichiometric ratio, epoxy to amine hydrogen groups equal to 1. The TP was polyetherimide, PEI Ultem 1000 supplied by General Electric. The structures are shown in Figure 1. Blends with concentration higher than 30 wt % of TP (33, 48, and 64 wt % of PEI) were prepared using a corotating twin screw extruder in a one-stage process.[8]

Dynamic mechanical measurements were made using a Rheometric RDA II in both laboratories using 25 mm plates, 1.5 mm gap, strain <3% at 10 rad/s in a temperature-controlled chamber.

Frequency-dependent complex dielectric measurements were made using an impedance analyzer controlled by a microcomputer. In the work discussed here, measurements at frequencies from hertz to megahertz are taken continuously throughout the entire cure process at regular intervals and converted to the complex permittivity, $\epsilon^* = \epsilon' - i\epsilon''$. The measurements are made with a geometry-independent interdigitated electrode.[10−11] The sensor is inserted into the blend and the

10.1021/ma991363q CCC: $19.00
Published on Web 04/25/2000

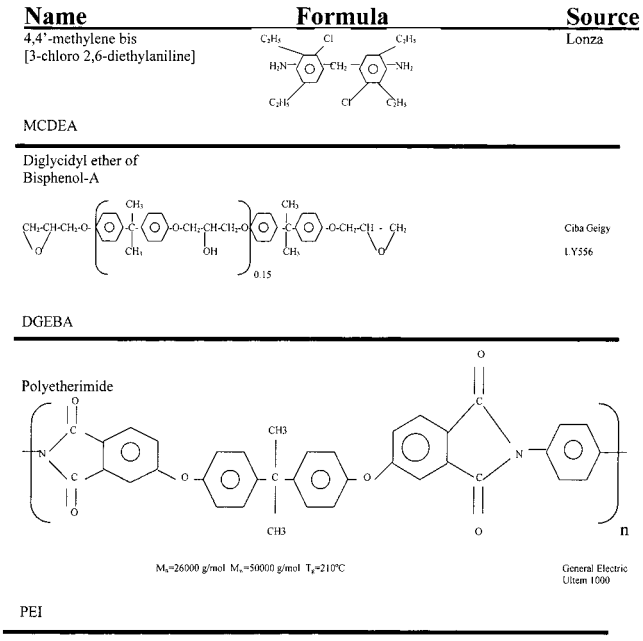

Figure 1. Structures of thermoset/thermoplastic system.

impedance is measured with either a Hewlett-Packard or a Schlumberger impedance bridge. This system permits multiplexed measurement of sensors. The sensor itself is planar, 1 × $^1/_2$ in. in area and 5 mm thick. This sensor-bridge microcomputer assembly is able to make continuous uninterrupted measurements of both ϵ' and ϵ'' over 10 decades in magnitude at all frequencies. The sensor is inert and has been used at temperatures exceeding 400 °C and a pressure over 1000 psi.[10]

Background

Frequency dependent measurements of the dielectric impedance of a material as characterized by its equivalent capacitance, C, and conductance, G, are used to calculate the complex permittivity, $\epsilon^* = \epsilon' - i\epsilon''$, where $\omega = 2\pi f$, f is the measurement frequency and C_o is the equivalent air replacement capacitance of the sensor.

$$\epsilon'(\omega) = \frac{C(\omega)\ \text{material}}{C_o}$$

$$\epsilon''(\omega) = \frac{G(\omega)\ \text{material}}{\omega C_o} \qquad (1)$$

This calculation is possible when using the sensor whose geometry is invariant over all measurement conditions. Both the real and the imaginary parts of ϵ^* can have dipolar (d) and ionic (i) charge components.

$$\epsilon' = \epsilon'_d + \epsilon'_i$$

$$\epsilon'' = \epsilon''_d + \epsilon''_i \qquad (2)$$

Plots of the product of frequency (ω) multiplied by the imaginary component of the complex permittivity $\epsilon''(\omega)$ make it relatively easy to visually determine when the low-frequency magnitude of ϵ'' is dominated by the mobility of ions and when at higher frequencies the rotational mobility of bound charge dominates ϵ''. Generally, the magnitude of the low-frequency overlapping values of $\omega\epsilon''(\omega)$ can be used to measure the change with time of the ionic mobility through the parameter σ where

$$\sigma(\Omega^{-1}\,\text{cm}^{-1}) = \epsilon_o \omega \epsilon''_i(\omega)$$

$$\epsilon_o = 8.854 \times 10^{-14} C^2\,\text{J}^{-1}\,\text{cm}^{-1} \qquad (3)$$

The changing value of the ionic mobility is a molecular probe which can be used to monitor changes in the viscosity during cure. The dipolar component of the loss at higher frequencies can then be determined by subtracting the ionic component.

$$\epsilon''(\omega)\ \text{diplolar} = \epsilon''(\omega) - \frac{\sigma}{\omega\epsilon_o} \qquad (4)$$

The peaks in ϵ'' dipolar (which are usually close to the peaks in ϵ'') can be used to determine the time or point in the cure process when the "mean" dipolar relaxation time has attained a specific value $\tau = 1/\omega$. The dipolar mobility, as measured by the mean relaxation time τ, is monitoring the α-relaxation process associated with vitrification, and it can be used as a molecular probe of the buildup in T_g. For example, the time of occurrence of a given dipolar α-relaxation time as measured by a peak in a particular high-frequency value of $\epsilon''(\omega)$ can be quantitatively related to the attainment of a specific value of the glass transition temperature.[10−13]

Interfacial polarization processes which occur in heterogeneous dielectrics will be present at the onset of phase separation, that is beginning at the onset of the transition from a homogeneous to a heterogeneous two-phase system.[4−7,29−40] These effects arise at the interface of two media having differing permittivities and conductivities. These interfacial effects can be quite strong sometimes creating increases in ϵ' by factors of 10 and a charge polarization relaxation time. The effect is dependent on the magnitude of the conductivity difference ($\sigma_2 - \sigma_1$) between the occluded phase σ_2, and the continuous phase, σ_1.

The most well-known theoretical model of this effect is the Maxwell−Wagner−Sillars model.[39,40] Using the Maxwell−Wagner−Sillars model, the complex dielectric permittivity of the mixture $\epsilon^*(\omega)$, of orientated occluded ellipsoids with complex dielectric constant, $\epsilon^*_2(\omega)$, at a volume fraction ν_2 dispersed in a continuous matrix with a complex dielectric constant, $\epsilon^*_1(\omega)$, can be calculated from the following equation:

$$\epsilon^* = \epsilon^*_1 \frac{\epsilon_1^*(1-\nu_2)(1-A) + \epsilon_2^*[\nu_2 + A(1-\nu_2)]}{\epsilon'_1 + A(1-\nu_2)(\epsilon_2^* - \epsilon_1^*)} \qquad (5)$$

Here $A(0 \le A \le 1)$, is the depolarization factor of the ellipsoidal filler particles. It depends on the shape of the particles (length of the long a to b short axis ratio for spheroids) and of the orientation of the field relative to the particle. For prolates spheroids (rod or needlelike) oriented along the shorter axis, A lies between 0 and $^1/_3$, while for oblates spheroids (disklike) oriented on the shorter axis, A lies between $^1/_3$ and 1. For spheres $A = {}^1/_3$.

Separating the real and imaginary parts leads to Debye's equations

$$\epsilon' = \epsilon_\infty + \frac{\epsilon_s - \epsilon_\infty}{1 + (\omega\tau)^2} \qquad (6)$$

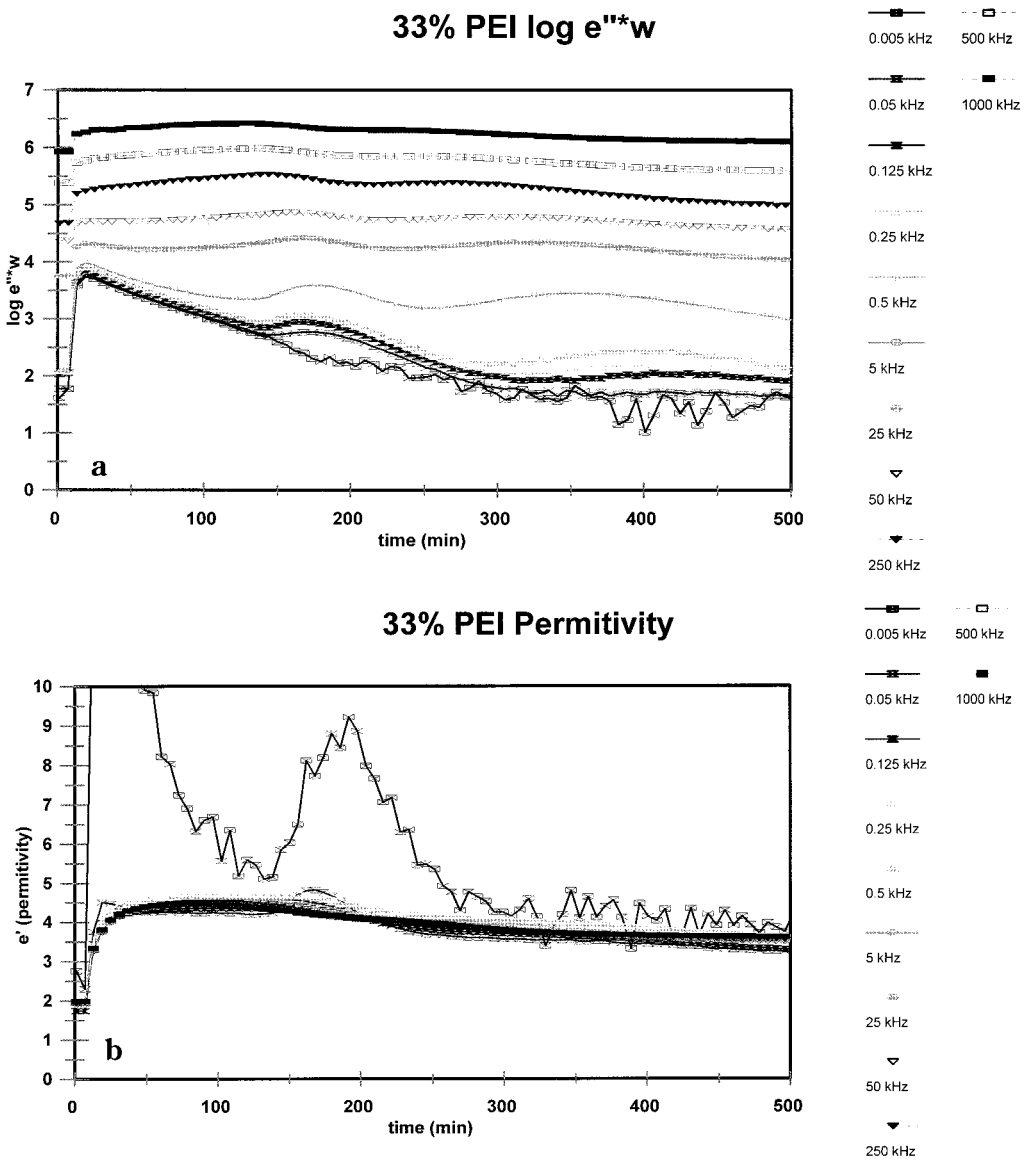

Figure 2. Plots of $\log(\epsilon''\omega)$ vs time and $\log \epsilon'$ vs time for the 33% PEI/epoxy−amine blend during the 135 °C cure.

$$\epsilon'' = (\epsilon_s - \epsilon\infty)\frac{\omega\tau}{1 + (\omega\tau)^2} \tag{7}$$

where $\omega = 2\pi f$ with explicit formulas for the low- and high-frequency limiting permittivity ϵ_s and ϵ_∞ and τ_{MWS}, the relaxation time of the interfacial charge polarization.

$$\tau_{MWS} = \epsilon_0\frac{\epsilon_1 + A(1 - \nu_2)(\epsilon_2 - \epsilon_1)}{\sigma_1 + A(1 - \nu_2)(\sigma_2 - \sigma_1)} \tag{8}$$

$$\epsilon_S = \epsilon_1\frac{\sigma_1 + [A(1 - \nu_2) + \nu_2](\sigma_2 - \sigma_1)}{\sigma_1 + A(1 - \nu_2)(\sigma_2 - \sigma_1)} + \nu_2\sigma_1 \times \frac{[\sigma_1 + A(\sigma_2 - \sigma_1)](\epsilon_2 - \epsilon_1) - [(\epsilon_1 + A(\epsilon_2 - \epsilon_1)](\sigma_2 - \sigma_1)}{[\sigma_1 + A(1 - \nu_2)(\sigma_2 - \sigma_1)]^2} \tag{9}$$

where ϵ_0 denotes permittivity of free space, σ_1 and σ_2 are the conductivities of each phase, and ϵ_1 and ϵ_2 are the limiting low-frequency permittivities for which by definition $\epsilon'' = 0$.

Results and Discussion

The neat epoxy−amine and three mixtures of 33%, 48%, and 64 wt % PEI, ϕ(TP), with the epoxy−amine thermoset precursor were cured at 135 °C. During the course of the cure the complex dielectric permittivity was measured over the 5 Hz to 1 MHz frequency range. The concentration of the epoxy−amine in the 64% PEI mixture was so low that the low loss properties of the PEI dominated the dielectric behavior and the changing dielectric behavior of the epoxy−amine during cure could not be detected. Dynamic mechanical measurements of the viscosity were also made during the cure process of the three blends. For the neat epoxy−amine system the viscosity was quite low, and a cone and plate viscometer was needed to monitor the viscosity.

In previous papers, a detailed discussion of the measured and model predicted extent of reaction in each of the blends has been presented.[8,9] As reported previously, the glass transition temperature data for each phase is used to estimate the composition and to predict the extent of reaction in that phase. These results along with viscosity are used in this analysis of measurements

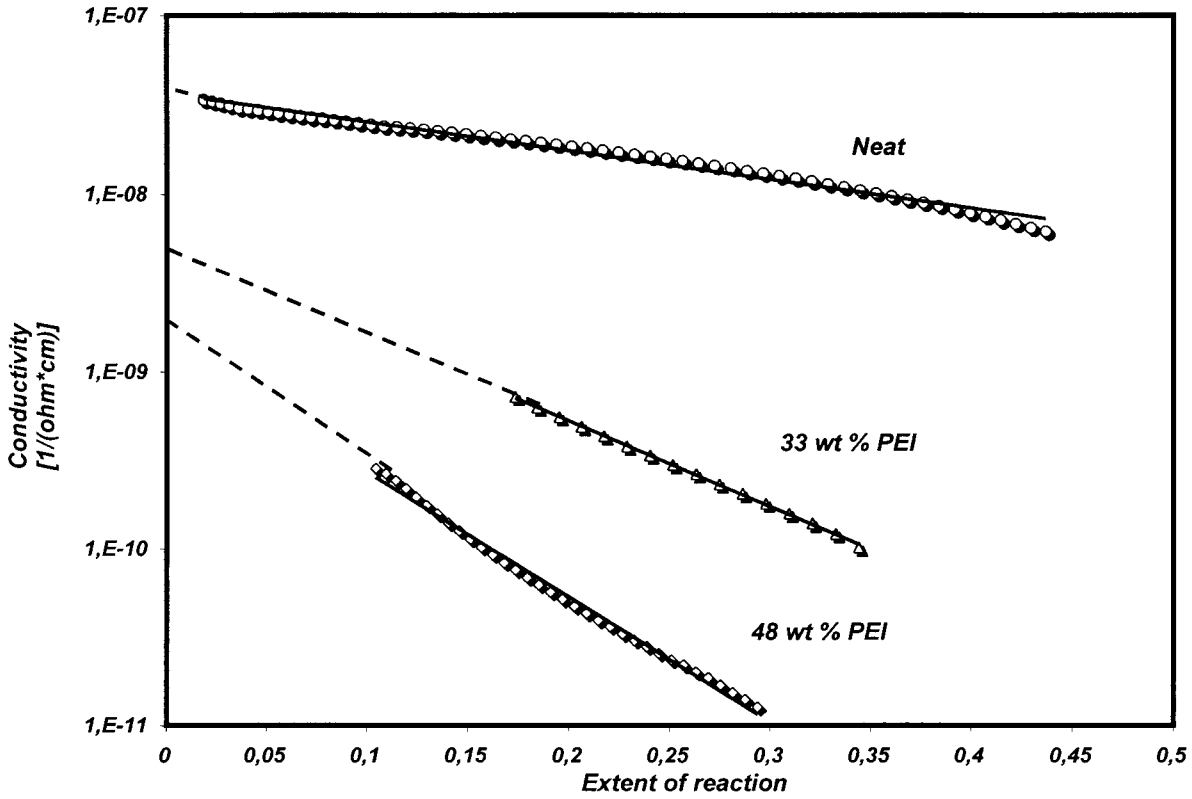

Figure 3. Plot of log conductivity vs extent of reaction before phase separation during 135 °C cure.

of the changes in the dielectric properties with time during the cure process.

Figure 2 displays for the 33% PEI blend the real ϵ' and loss component ϵ'' of the permittivity scaled by the frequency with time during isothermal cure at 135 °C. The value of ϵ' shows a sharp rise at 128 min indicating the onset of phase separation. The imaginary loss, component ϵ'' shows overlapping values at the lower frequencies. These values of ϵ'' can be used to determine a frequency independent conductivity using eq 3.

Two sets of peaks in ϵ'' occur. The first set occurs both before and after phase separation. They occur at the higher frequencies before phase separation and at the lower frequencies after phase separation. A second set of peaks starting at the higher frequencies occur only after phase separation. These peaks can be used to determine the achievement of an effective relaxation time τ where $\tau = (2\pi f)^{-1}$ at the time of a peak in $\epsilon''(\omega)$ at that frequency, f. In the following discussion these dielectric quantities and the viscosity will be measured and analyzed along with the previously reported values of extent of reaction x and the values of T_g to both understand the dielectric behavior of a reactive TP/TS blend and to build a fundamental basis from which the transformations of the reactive TP/TS blend can be monitored in situ during polymerization−fabrication using dielectric measurements.

Before Phase Separation. The TP/TS blend is a homogeneous mixture in which one observes, at different levels of TS precursor dilution, the changing conductivity of the epoxy−amine *i*-mers as the viscosity and the extent of reaction increases. Equation 3 was used to calculate the conductivity from the dielectric data. In Figure 3, the values of $\log(\sigma(t))$ are plotted vs the extent of reaction $x(t)$, reported previously.[8,9] The results in Figure 3 show a decrease in the initial conductivity and throughout the reaction which will be shown cannot

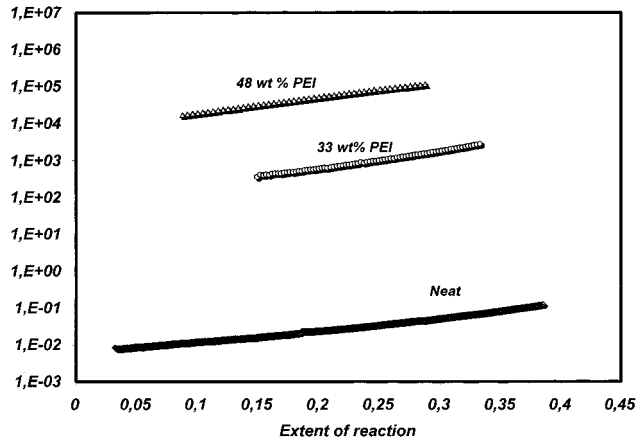

Figure 4. Plot of log viscosity vs extent of reaction before phase separation during 135 °C cure.

be explained by the change in concentration and viscosity of the TS in the TP. Equally pertinent, the results show an increasing rate of decrease in $\sigma(t)$ with extent of reaction, $x(t)$, as the percentage of thermoplastic increases. First to examine the role of viscosity, Figure 4 displays $\log(\eta)$ vs extent of reaction before phase separation. There is an approximate linear shift in the viscosity with the thermoplastic weight percent and the rate of change in η with reaction extent is approximately the same for all the homogeneous blends as well as the neat system. These viscosity results are as expected. They differ significantly from the relation of the conductivity to the extent of reaction as shown in Figure 3.

In Figure 5 a log−log plot of the relationship of conductivity to viscosity for the neat, the 33% PEI, and the 48% PEI in the homogeneous blend is displayed. The slopes b of $\log \sigma(t) = b \log \eta(t)$ are reported in Table 1. Overall these results, as seen in Figures 3−5 and Table

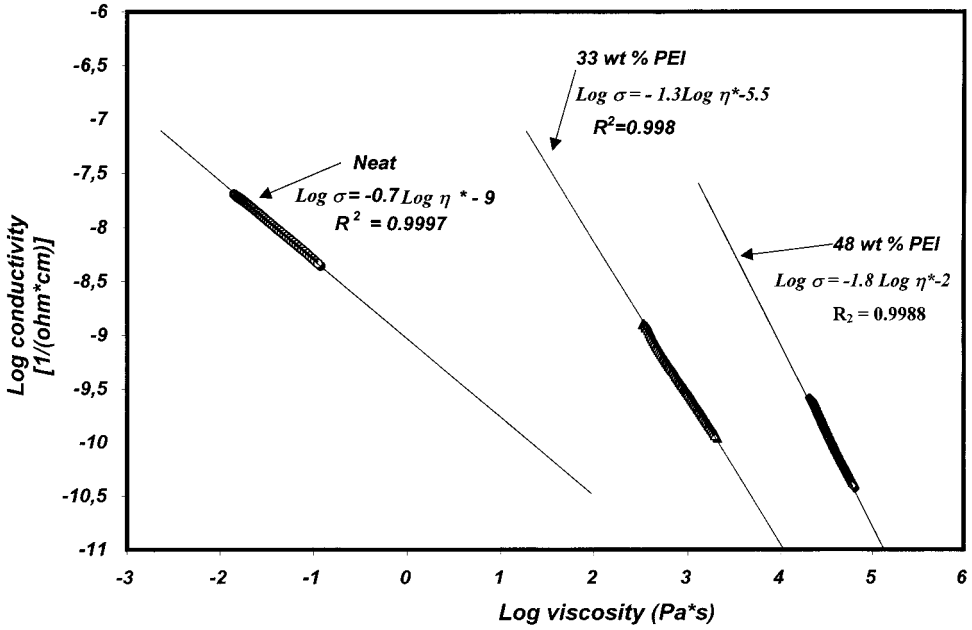

Figure 5. A log−log plot of conductivity vs viscosity during 135 °C cure.

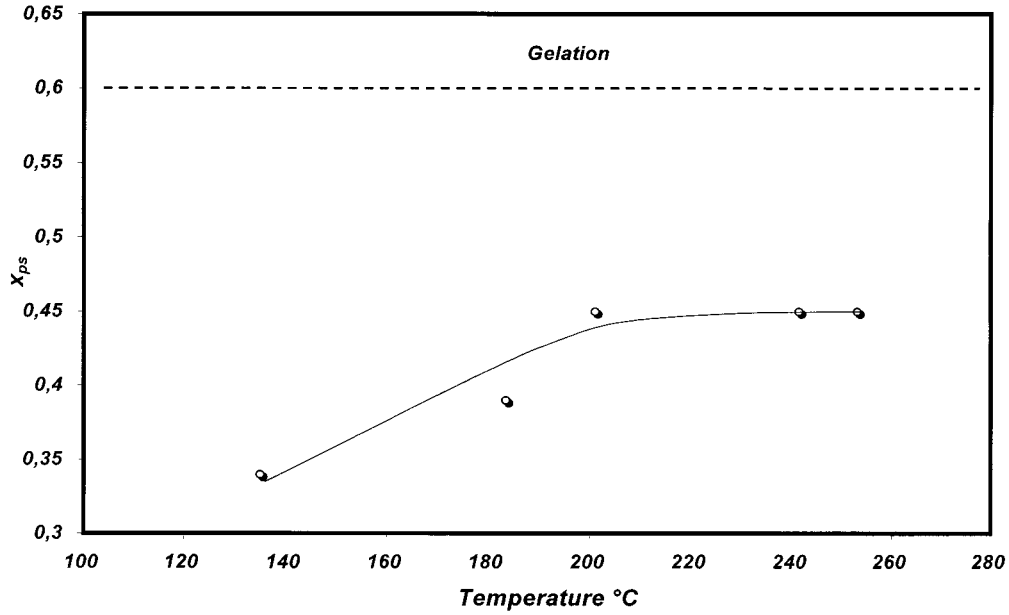

Figure 6. Extent of reaction at onset of phase separation vs isothermal cure temperature. Extent of reaction at gel is dashed top line.

Table 1

	slopes		
% PEI	log(σ)vs x	log(η) vs x	log σ vs log η
0	−1.6	3.2	−0.7
33	−4.9	4.8	−1.3
48	−6.9	3.9	−1.8

1, show that the conductivity is affected significantly by factors other than viscosity and concentration. As such, the results provide insight into the fundamental conduction mechanism. If conduction in epoxy−amine systems during cure was due only to viscosity controlled translation diffusion of impurity ions such as Cl^- (which could originate from the epichloro epoxy precursors) or other ions of constant concentration, the conductivity viscosity/concentration ratio would be expected to be approximately constant. The fact that there are significant changes in the value of this ratio as seen from the slopes of Figures 3−6 and summarized in Table 1 suggests other factors are present. For these curing systems we suggest that a major conduction mechanism involves hydrogen bond exchange. This mechanism of exchange would most likely involve the amine group and hydroxy groups formed during the polycondensation reaction. Such a mechanism requires a structure and number of those bonds such that H-bonding and proton transfer is facilitated. The increasing rate of decrease in conductivity with viscosity as the thermoplastic concentration increases supports this view that the structure and number of H-bonding proton exchange groups in the reactive mixture of epoxy, amine, and polymer products in the presence of higher concentrations of TP has a much larger effect on the magnitude of the conductivity than does the increase in the viscosity.

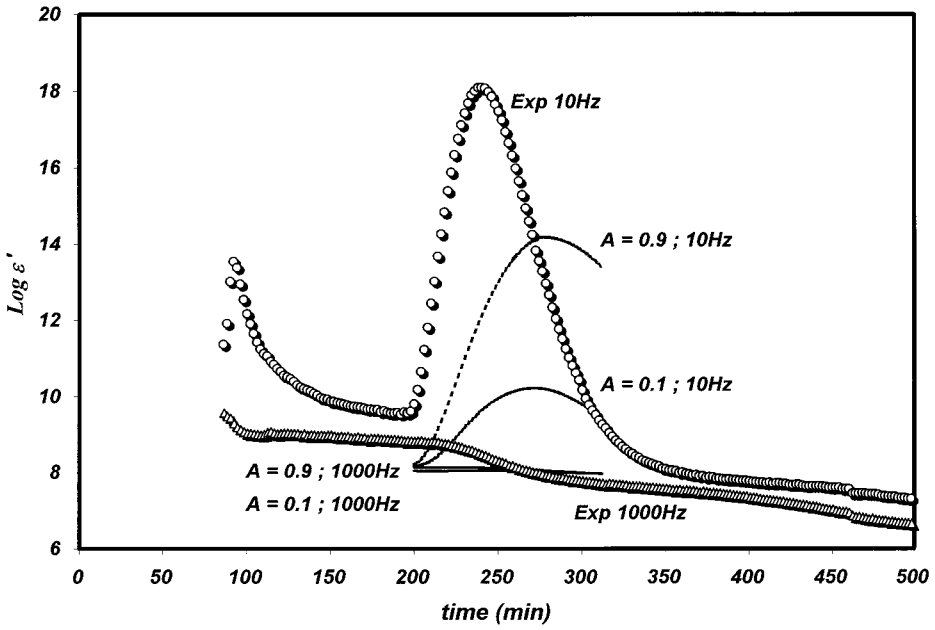

Figure 7. Plot of log ϵ' experimental during phase separation and theoretical values based on MWS theory for aspherical shape factors of $A = 0.9$ and $A = 0.1$ at 10 and 1000 Hz during 135 °C cure.

When the relative proximity and number of such bonds remains constant, the conductivity in general will track the change in viscosity. This observation which is reported in the cure of neat TS by many authors over the past decade has led to the wide use of dielectric measurements of conductivity as an in situ means of monitoring the changing viscosity up to the vicinity of gelation.[10−28] The current results strongly suggest that a major molecular mechanism for the conductivity in these pure epoxy−amine systems is a hydrogen bond exchange mechanism. They suggest that the slope of the conductivity-viscosity relation before phase separation and up to gel may be, in part, a function of the number and geometric structure of proton donor acceptor bonds in the monomers and the resulting chains. These observations further support the explanation for the seemingly anomalous rise in the conductivity previously observed in certain epoxy systems and the proposed explanation that the proton group proximity for these systems increases during the later stages of cure.[23]

The Onset of Phase Separation. It is characterized by the creation of an interface between forming phases. From the point of view of dielectric behavior, the initial onset of the phase separation process has the potential to generate a large change in the permittivity ϵ' since interfacial surfaces with charge separated by molecular distances represent a large increase in capacitance i.e., $C_o \approx$ area/distance. Furthermore, once the phase separation process has generated an occluded phase of conductive epoxy-rich *i*-mers, the α phase, surrounded by a PEI-rich nonconducting continuous phase, there is the potential as previously described for Maxwell−Wagner−Sillers relaxation effects, eqs 5−9. Figure 2 (33 wt % PEI) clearly shows a large sudden increase in the value of ϵ' at 128 min. Another sample showed this rise at 105 min. The cloud point was observed at 118 min. For the 48% PEI blend the sharp rise in ϵ' occurred at 211 and 202 min in two separate runs. For the 48% PEI system the cloud point was observed at 235 min. Rheological measurements showed the phase separation transition at 113 min for 33% PEI and 216 min for 48% PEI. Clearly as summarized in Table 2 the onset of the dielectric interfacial polarization, as seen by a sharp rise in ϵ', is a good instrumental means to monitor in situ with a capacitance sensor the onset of the phase separation process.

Table 2. Comparison of Detected Times (min) of Phase Separation

	33 wt %	48 wt %
dielectric	115	205
cloud point	118	235
DSC	118	235
rheology	113	216

Table 3

temperature, °C	xps
135	0.34
183	0.39
201	0.45
241	0.45
253	0.45

The Effect of the Cure Temperature on the Onset Time for Phase Separation Examined Using the Observed Large Increase in ϵ'. Dielectric monitoring was conducted on the 33% PEI blend cured isothermally at 183, 201, 241, and 253 °C as well as at 135 °C. The time for phase separation was determined from the observed onset of the large MWS increase in ϵ''. The extent of reaction was calculated vs that time for each of these isothermal conditions using the previously developed kinetics.[8,9] Table 3 reports values of the extent of reaction $x(t_{ps})$ at phase separation. Figure 5 displays the value of $x(t_{ps})$ vs temperature. The results show that as the temperature goes up the reaction advances to a higher level before the phase separation process begins, reflecting the higher level of solubility of the TS oligomer in the PEI with increasing temperature and confirming a UCST behavior for the blend.[41] However this effect decreases as the value of $x(t)$ increases representing larger and more branched oligomers due to competing activation energy controlled processes of nucleation and the reaction rates.[42] An upper value of $x(t_{ps}) = 0.45$ is reached near 200 °C.

Relaxation Peaks. They are observed in Figure 2 both before, during and after the onset of phase separation. The focus of this discussion is an analysis of these dipolar peaks and their basis as a consequence of the phase separation MWS process, the buildup in T_g of the PEI-rich continuous β phase and the buildup in T_g of the epoxy-rich occluded α phase.

Equations 7−9 can be used to calculate the effect with time of the MWS phase separation process on ϵ' and ϵ'' compared to the experimental values. The values of ϵ_1, ϵ_2, σ_1, and σ_2 can be calculated from the existing time dependent data of the neat, 33% and 48% PEI blends and the known concentration changes within each phase with time measured form the previously reported T_g data. Thus, the composition and degree of advancement in each phase is calculated and thereby the conductivity can be calculated for each phase, i.e., $\sigma_1(t)$ and $\sigma_2(t)$. ϵ_s is calculated in a similar way. The value of ϵ_∞ is found to be small and approximately constant with composiiton and advancement. To assess the shape of the α-phase micelles, two different values of the ellipsoidal shape factor $A = 0.9$, oblate, and $A = 0.1$, prolate, recalling $A = 0.33$ is for spherically shaped particles, were used in calculations of ϵ' and ϵ'' at 10 and 1000 Hz. The theoretical MWS predicted and the experimental values are shown in Figure 7. The 1000 Hz MWS values of ϵ'' and ϵ' for $A = 0.1$ and $A = 0.9$ lie on top of each other in Figure 7 and are seen as one line. The MWS model predicted results compared to the experimental data in Figure 7 suggest that the occluded particles tend toward a nonspherical oblate ellipsoidal shape. TEM micrographs were examined at three different extents of reaction as shown in Figure 8. The TEM photos show a high degree of asphericity which decreases with reaction time. We view these photos with caution however. The TEM's may not accurately reflect the shape at this extent of reaction during cure because it is observed after cooling when the extents of reaction is low and the particles can be easily deformed. Overall we are surprised by these results and continue to view them with questions as we would expect the particles to be spherical originating from nucleation and growth.

From the beginning, before, during, and after the onset of phase separation, the epoxy groups in the homogeneous phase and in both the β and α phases continue to react. With increasing extent of reaction more epoxy *i*-mers become insoluble in the PEI and diffuse in to the α, occluded epoxy-rich phase. As the TS *i*-mers diffuse out of the β phase, the β phase becomes richer in PEI. As a result the T_g of the continuous β phase increases. Since T_g of the neat PEI is well above the 135 °C cure temperature, a point in time is reached where the increase in weight percent of PEI in the β phase causes the T_g of the β phase to approach 135 °C. At this time, the β phase enters into the glassy state and the epoxy−amine oligomer diffusion process into the α phase is quenched. Throughout this time and continuing after achievement of the glassy state in the β phase, the TS *i*-mers in the occluded α phase continues to react. As in the β phase, but due to reaction advancement, the T_g of the α phase increases until its T_g also reaches 135 °C. Again once this buildup in T_g in the α phase has occurred, the α phase reaction is quenched by formation of a glass. Post cure at a higher temperature can of course increase T_g of both phases up to completion of the epoxy reaction in both the α and β phases.

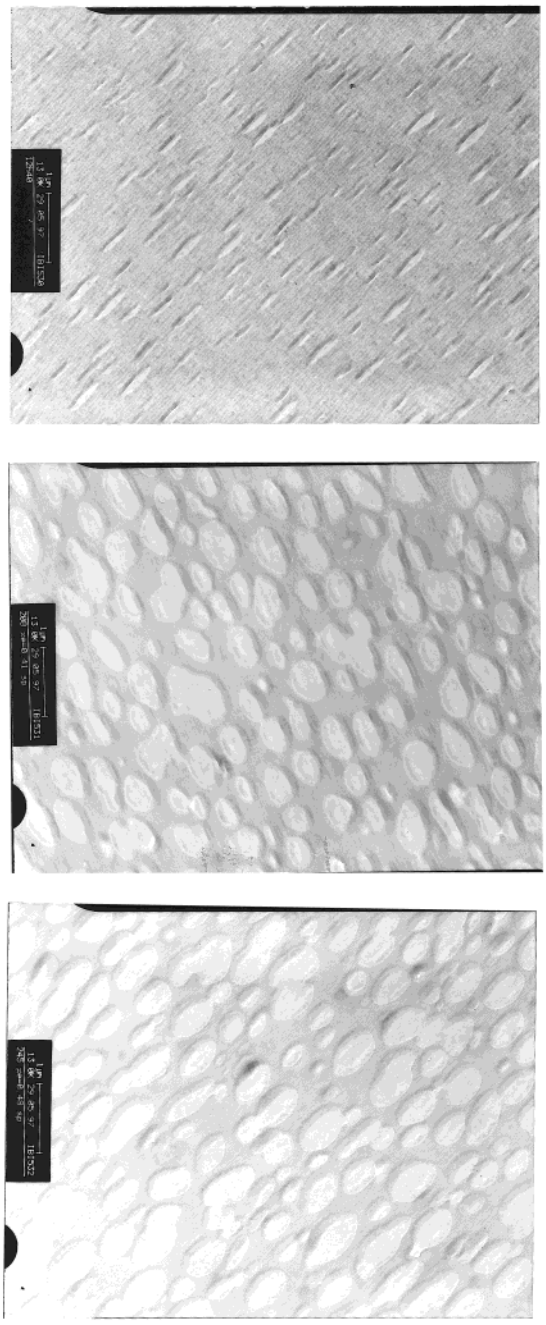

Figure 8. TEM photos of 33% PEI system just after phase separation at $x = 0.34$ (top), $x = 0.41$ and $x = 0.48$ (bottom) during 135 °C cure. Solid symbols are 33% PEI; open symbols are 48% PEI.

The buildup in the glass transition temperature is accompanied by rapid increase in viscosity and a corresponding long range cooperative relaxation process, the T_g α relaxation. The T_g α-relaxation time, characterizing the preglass, highly viscous state, is observed in both mechanical and dielectric relaxation experiments. The advantage of the frequency dependent dielectric measurements to monitor this process is that they cover a much larger range in time, over 6 decades in frequency, from Hz to MHz, while conventional mechanical experiments cover about 2 decades in the Hz region. The dielectric data in Figure 1 shows two distinct series of relaxations, the first occurring over 120−180 min and the second over 300−360 min.

Figure 8 displays values of the extent of reaction in each of these two regions for the 33%, the 48% and the

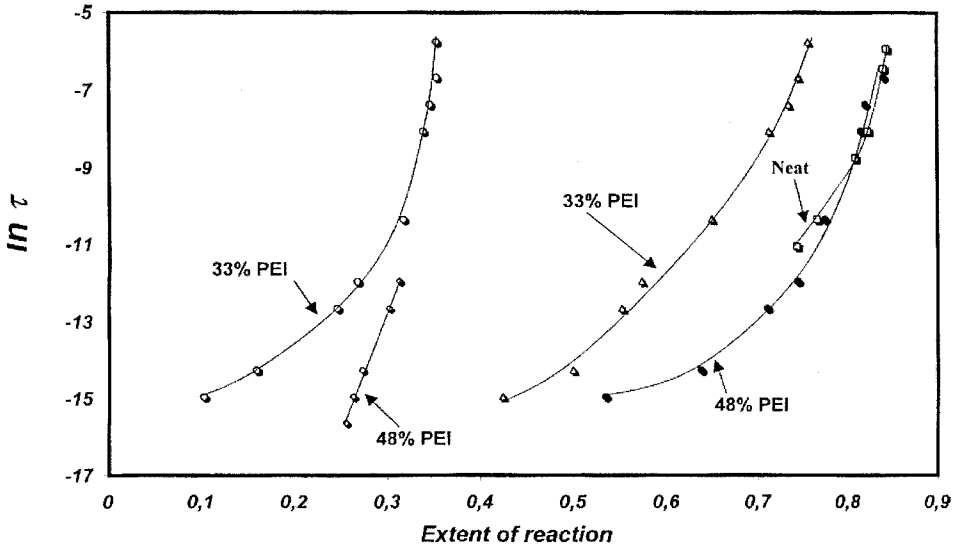

Figure 9. Plot of ln(relaxation time) vs extent of reaction before phase separation (x) and after phase separation in the α epoxy-rich occluded phase (x_α) for the 33% and 48% PEI blends and the neat epoxy−amine during 135 °C cure.

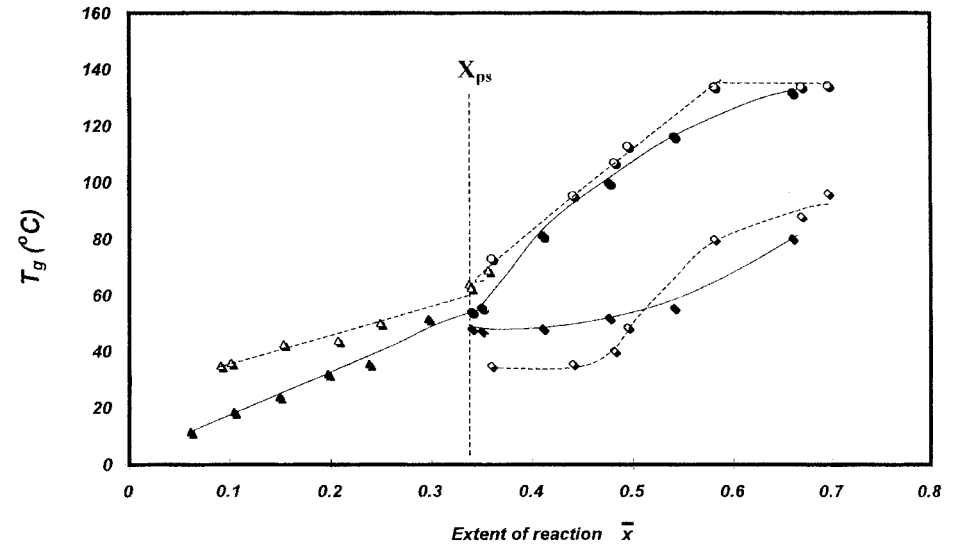

Figure 10. Experimentally determined values of T_g vs extent of reaction for the 33% system, solid symbols, and the 48% system, open half-filled symbols, during 135 °C cure.

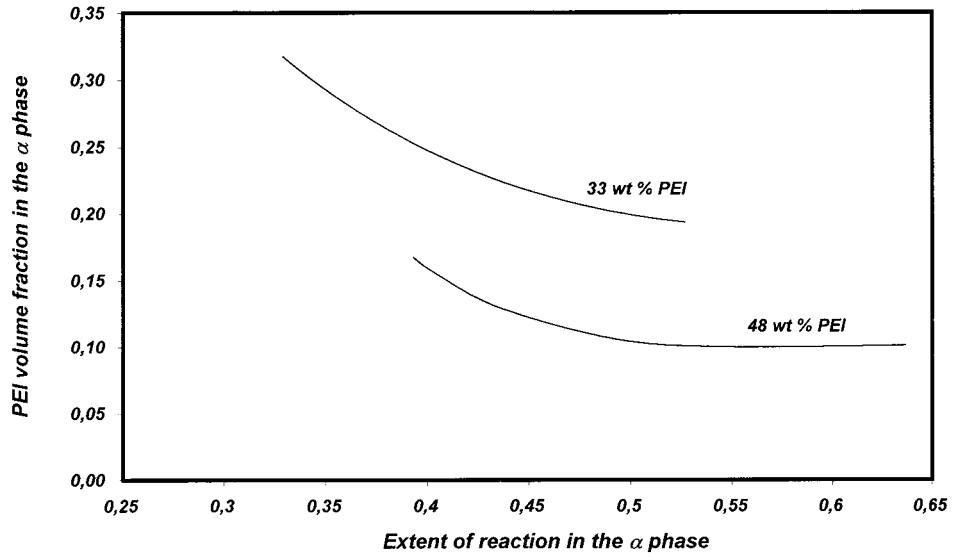

Figure 11. PEI volume fraction in the α phase occluded particles determined from the measured values of T_g as described in ref 8 during 135 °C cure.

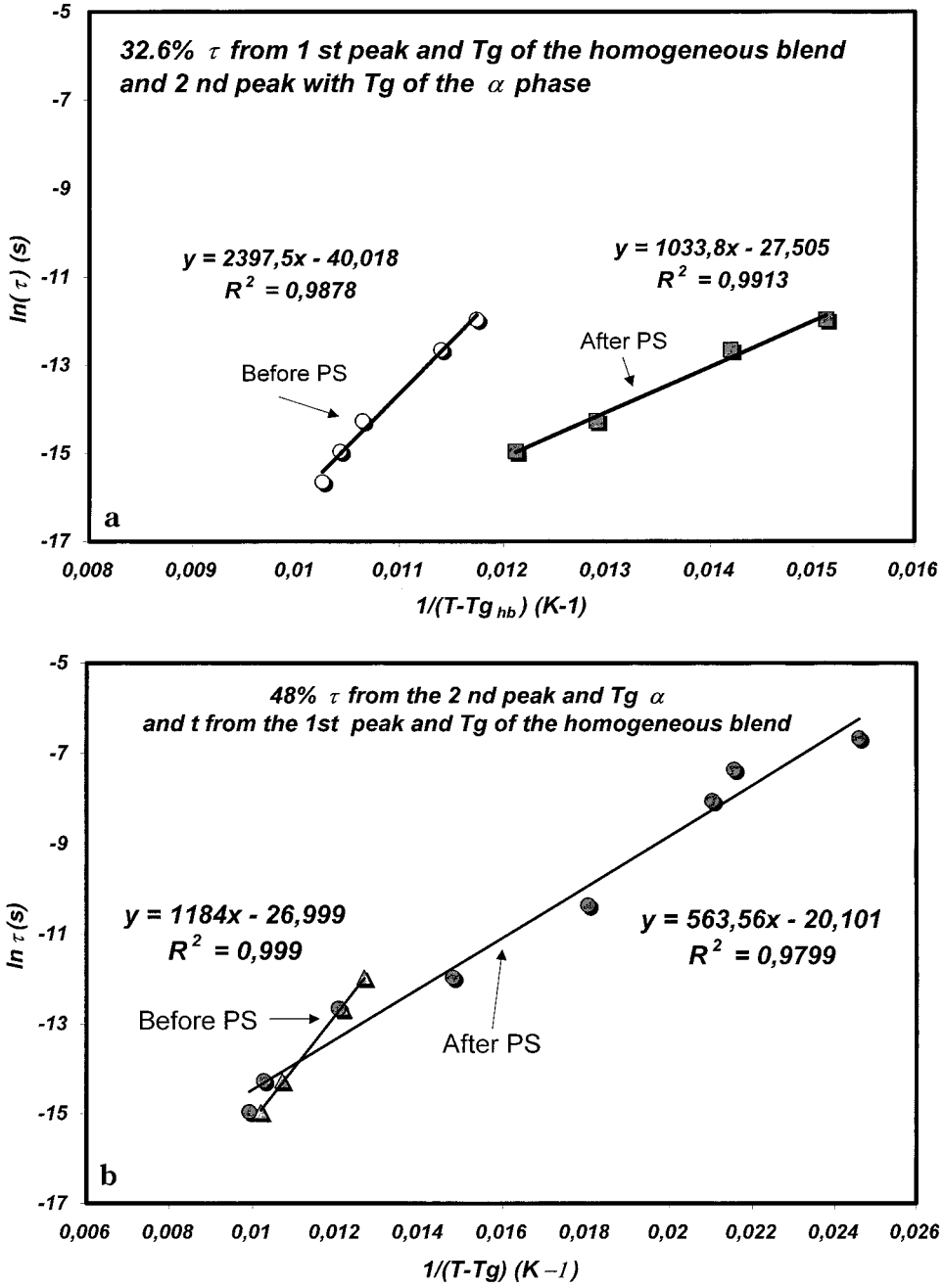

Figure 12. $(T - T_g)^{-1}$ temperature dependence of the α-relaxation time τ for (a) the 33% PEI blend and (b) the 48% PEI blend.

neat epoxy system at the time the relaxation time associated with the peak in a particular frequency measurement of ϵ'' occurs. As described, there are two relaxation regions. The first occurs during the early part of the reaction before phase separation during which time there is a buildup in T_g of the homogeneous phase as the epoxy reacts. These T_g−relaxation peaks are displayed for $x < 0.35$ before the onset of phase separation, region of the plot. The absence of the lower frequency peaks for $x > 0.35$ after the onset of phase separation, suggests that with the onset of phase separation, the relaxation time and the increase in T_g of the β phase occurs very rapidly. As a result, these slower relaxation time peaks are undoubtedly mixed in with the MWS peak previously described. This is one possible cause for the inability of the MWS predicted relaxation spectrum to completely match the experimental data.

After phase separation, a second set of T_g α-relaxation peaks are observed beginning with the high frequencies. These are the result of the increasing extent of epoxy amine reaction in the α-occluded phase particles. Figure 8 shows the experimentally determined values of τ in the 33% and 48% systems vs extent of reaction before phase separation, x, and after phase separation in the x phase x_α. Also included are values for the neat epoxy amine system. Figure 8 shows the 48% and neat epoxy values of τ are in close agreement, indicating the composition of the α-phase in the 48% blend contains very little PEI concentration. Figure 9 shows the experimentally determined T_g values before and after phase separation in the 33% and 48% blends. The presence of PEI in the α-phase, as in the β phase, increases T_g for a given value of $x(t)$ because the T_g of PEI (210 °C) is much higher. Figure 10 shows the T_g experimentally determined change in epoxy concentra-

tion of the occluded epoxy-rich particles with time in both the 33% and 48% systems calculated from the evolution of T_g.[8] These results clearly show that the basis for the overlap of α-relaxation peaks in the 48% system vs time with the neat epoxy system is due to the low percent of TP in these particles. For the 33% PEI blend the peaks occur at much lower values of x_α, indicating a significant percentage of PEI in the α phase, which is again supported by Figure 10. Overall the results show that the time of occurrence of these peaks is a measure of their composition.

It is interesting to note that the actual elapsed time after phase separation for the α-relaxation peaks to appear, is nearly the same for the 33% compared to the 48% system. This suggests that the dilution effect slowly down reaction rate in the 33% epoxy α phase is more or less compensated by the more rapid increase in T_g (α) as a result of the higher PEI content.

Finally in Figure 11 we examine the $(T - T_g)^{-1}$ temperature dependence of the α relaxation peaks. Previous work on epoxy−amine/orthophenyl blends has shown that at high extents of reaction approaching completion the apparent activation energy decreases and is lowest for the neat epoxy system compared to the blends.[41] The reverse is true at other extents of reaction where the apparent activation energy does not vary much with reaction extent. Here an increase in the percent of orthoterpheny decreased the apparent activation energy. These observations are consistent with the results reported in Figure 11. The lowest apparent activation energy is observed at the high extent of reaction for the almost pure epoxy α phase occluded particles in the 48% system. For the prephase low extent of conversion α-relaxation peaks, the results again agree with the *o*-terphenyl epoxy amine system as the 48% system, richer in TP, has a lower apparent activation energy than the 33% system.

Conclusions

Frequency-dependent dielectric measurements are an excellent technique for monitoring the complex chemical, composition and morphological changes occurring during cure of high-temperature *T*P/TS blends. The T_g α-relaxation peaks can be used to monitor the buildup in T_g and thereby reaction advancement in the homogeneous phase before phase separation and in the occluded phase after phase separation.

The onset of phase separation is readily detected by a sharp MWS charge polarization rise in ϵ'. The dielectric detected time is in close agreement with mechanical and cloud point techniques. Using this method to detect the time of phase separation at different temperatures showed the magnitude of the reaction advancement at the onset of phase separation increases with higher temperature due to a higher solubility in the PEI, but appears to achieve a maximum value at about $x = 0.45$. The MWS predicted values of ϵ'' were in relatively good agreement with the experimental values and suggest the occluded particles have a non spherical shape.

The conductivity, in these blends does not follow the generally expected inverse viscosity power dependence and decreases much more rapidly then expected based on the concentration of thermoplastic and the change in viscosity. The results support a hydrogen bond exchange mechanism which is strongly affected by the concentration-proximity of the proton exchange groups.

Acknowledgment. Support from CNRS and fruitful discussions with G. Boiteux and G. Seytre in France, along with funding from the NSF Foundation INT 97226207 and NSF Center of Excellence at VPI MR 912004.

References and Notes

(1) Williams, R. J. J.; Rozenberg, B. A.; Pascault, J. P. .Reaction-induced phase separation in modified thermosetting polymers. *Adv. Polym. Sci*. **1996**, 128, 95.
(2) Girard-Reydet, E.; Sautereau, H.; Pascault, J. P.; Keates, P.; Navard, P.; Thollet, G.; Vigier, G. *Polymer* **1998**, *39*, 2269−2280.
(3) Pearson, R. A. Rubber toughened plastics I. *Adv. Chem. Ser. ACS* **1993**, *233*, 407−425.
(4) Vanderbosch, R. W.; Meijer, H. E. E.; Lemstra, P. J. *Polymer* **1995**, *36*, 2903.
(5) Eklind, H.; Maurer, F.; Stechman, P. *Polymer* **1997**, *38*, 1047.
(6) Venderbosch, R.; Meijer, H.; Lemstra, P. *Polymer* **1994**, *35*, 4349.
(7) Lemstra, P. J.; Kurja, J.; Meijer, H. E. E. In *Materials Science and Technology*; Cahn, R. W., Haasen, P., Kramer, E. J., Eds. *Processing of polymers*; Meijer, H. E. E., Ed.; Wiley VCH: Weinheim, Germany, 1997; Vol. 18, p 513.
(8) Bonnet, A.; Pascault, J. P.; Sautereau, H.; Taha, M.; Camberlin, Y. *Macromolecules* **1999**, v32, n25, p8517.
(9) Bonnet, A.; Pascault, J. P.; Sautereau, H.; Camberlin, Y. *Macromolecules* **1999**, *32*, 8524.
(10) Kranbuehl, D. *Dielectric Spectroscopy of Polymer Mats*; Runt, J., Ed.; American Chemical Society: Washington, DC, 1997; p 303.
(11) Kranbuehl, D. In *Encyclopedia of Composites*; Lee, S. M., Ed.; VCH: New York, 1989; pp 531−543.
(12) Senturia, S.; Sheppard, S. *J. Appl. Polym. Sci.* **1986**, *80*, 1−48.
(13) *Polymer Materials Science and Engineering*; May, C., Ed.; ACS Symposium Series 27; American Chemical Society: Washington, DC, 1983.
(14) Hedvig, P. *Dielectric Spectroscopy of Polymers*; Wiley: New York, 1977.
(15) Mijovic, J.; Belluci, F.; Nicolais, L. *Electrochem Soc.* **1995**, *142*, 1176−1182.
(16) Mijovic, J.; Winnie Tee, C. F. *Macromolecules* **1994**, *27*, 7287−7293.
(17) Bellucci, F.; Valentino, M.; Monetta, T.; Nico demo, T. L.; Kenny, J.; Nicolais, J.; Mijovic, J. *J. Polym. Sci., Part B: Polym. Phys.* **1995**, *33*, 433−443.
(18) Mangion, M. B. M.; Johari, G. P. *Macromolecules* **1990**, *23*, 3687−3695.
(19) Mangion, M.; Johari, G. *J. Polym. Sci., Polym. Lett. Ed.* **1991**, *29*, 1117−1125.
(20) Parthun, M. B.; Johari, G. *Macromolecules* **1992**, *25*, 3254−3263.
(21) Boiteux, G.; Dublineau, P.; Feve, P.; Mathieu, C.; Seytre, G.; Ulanski, J. *Polym. Bull.* **1993**, *30*, 441−447.
(22) Mathieu, C.; Boiteux, G.; Seytre, G.; Villain, R.; Dublineau, P. *J. Non-Cryst. Solids* **1994**, *172−174*, 1012−1016.
(23) Gallone, G.; Levita, G.; Mijovic, J.; Andjellics, Rolla, P. *Polymer* **1998**, *39*, 2095.
(24) Xu, X.; Galiatsatos, V. *Makromol. Symp.* **1993**, *76*, 137.
(25) Deng, Y.; Martin, G. *Macromolecules* **1994**, *27*, 5141−5146.
(26) Companik, J.; Bidstrup, S. *Polymer* **1994**, *35*, 4823−4840.
(27) Bidstrup, S.; Sheppard, N.; Senturia, S. *ANTEC* **1987**, 987−993.
(28) Bidstrup, W.; Bidstrup, S.; Senturia, S. *ANTEC* **1988**, 960−966.
(29) Lestriez, B.; Maazouz, A.; Gerard, J. F.; Sautereau, H.; Boiteux, G.; Seytre, G.; Kranbuehl, D. *Polymer* **1998**, *39*, 6733−6742.
(30) Poncet, S.; Boiteux, G.; Pascault, J. P.; Sautereau, H.; Seytre, G.; Rogozinski, J.; Kranbuehl, D. *Polymer* **1999**, *40*, 6811−6820.
(31) Alig, J. M.; Jenniger, W. *J. Polym. Sci., B: Polym. Phys.* **1998**, *36* 2461−2470.
(32) Brown, J. M.; Srinivasan, S.; Ward, T.; Loos, A. C.; Hood, D.; Kranbuehl, D. *Polymer* **1996**, *36*, 1691−1696.
(33) MacKinnon, A. J.; Jenkins, S. D.; MacGrail, P. T.; Pethrick, R. A. *Polymer* **1993**, *34*, 3252−3263.
(34) MacKinnon, A. J.; Jenkins, S. D.; MacGrail, P. T.; Pethrick, R. A. *Macromolecules* **1992**, *25*, 3492−3499.
(35) Delides, C. G.; Hayward, D.; Pethrick, A.; Vatalis, A. S. *Eur. Polym. J.* **1992**, *28*, 505−512.

(36) Maistros, G.; Block, H.; Bucknall, C. B.; Partridge, I. K. *Polymer* **1992**, *33*, 4470−4478.
(37) Korkakas, G.; Gomez, C. W.; Bucknall, C. B. *Plast., Rubber Compos. Process. Appl.* **1993**, *19*, 285.
(38) Kranbuehl, D.; Kim, T.; Liptak, S. C.; McGrath, J. E. *Polym. Prepr.* **1993**, *34*, 488−489.
(39) Sillars, R. W. J. *Inst. Electron. Eng.* **1937**, *80*, 378.
(40) Van Beek, L. H. K. Dielectric Behavior of Heterogeneous Systems. *Prog. Dielectrics* **1967**, *7*, 69−114.
(41) Riccardi, C. C.; Barrajo, J.; Williams, R. J. J.; Girard-Reydet, E.; Sautereau, H.; Pascault, J. P. *J. Polym. Sci., Part B: Phys.* **1996**, *34*, 349−356.
(42) Williams, R. J. J.; Barrajo, J.; Adabbo, H. E.; Rojas, A. J. In *Rubber-Modified Thermoset Resins*; Riew, C. K., Gillham, J. K., Eds.; Advances in Chemistry *208*, American Chemical Society: Washington, DC, 1984; pp 195−213.
(43) Andjelic, S.; Mijovic, J. *Macromolecules* **1998**, *31*, 2872−82.

MA991363Q